Journal of Power Sources 249 (2014) 367–372

Contents lists available at ScienceDirect

Journal of Power Sources

journal homepage: www.elsevier.com/locate/jpowsour

Aqueous rechargeable alkali-ion batteries with polyimide anode

H. Qin [1], Z.P. Song [1], H. Zhan*, Y.H. Zhou

Department of Chemistry, Wuhan University, Wuhan, Hubei 430072, China

HIGHLIGHTS

- Polyimide is proposed as the anode for ARLB and ARSB.
- Polyimide/$LiCoO_2$ cell has higher capacity and energy density than other ARLBs.
- Polyimide anode shows a good electrochemical performance in $NaNO_3$ solution.
- Using polyimide anode supplies an alternate, promising strategy for large-scale energy storage.

GRAPHICAL ABSTRACT

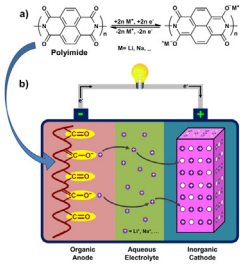

ARTICLE INFO

Article history:
Received 15 August 2013
Received in revised form
19 October 2013
Accepted 21 October 2013
Available online 1 November 2013

Keywords:
Polyimide anode
Aqueous rechargeable lithium-ion battery
Aqueous rechargeable sodium-ion battery
Cycling stability
Rate performance

ABSTRACT

1,4,5,8-Naphthalenetetracarboxylic dianhydride (NTCDA)-derived Polyimide is proposed as the anode material for aqueous rechargeable lithium-ion or sodium-ion battery (ARLB or ARSB), which is based on a mechanism beyond the intercalation chemistry. Comparing with other transient oxide anode for ARLB, Polyimide has more suitable working voltage, higher capacity and better structure stability. Therefore, the ARLB with Polyimide anode and $LiCoO_2$ cathode presents a specific capacity of 71 mAh g^{-1} and a specific energy of 80 Wh kg^{-1} in 5 M $LiNO_3$ solution at the current rate of 100 mA g^{-1}, which is the highest among all reported ARLB system. Besides, it shows excellent cycling stability and rate capability. The ARSB system is demonstrated by Polyimide/$NaVPO_4F$ cell. It has been proved that the Polyimide anode has a good capacity performance and cycling stability in 5 M $NaNO_3$ solution. The two aqueous rechargeable batteries with Polyimide anode both show a promising prospect in large-scale energy storage.

1. Introduction

"Aqueous rechargeable lithium-ion battery (ARLB)" [1,2] is an emerging battery technology, the concept of ARLB was first proposed because of the safety issue stemming from unavoidable using of flammable organic solvents in traditional nonaqueous Li-ion battery. After the first work on VO_2/$LiMn_2O_4$ ARLB system being reported by Dahn et al., in 1994 [1], many other ARLB systems have been studied [2–14]. Typically, the ARLB consists of aqueous electrolyte (e.g., $LiNO_3$ or Li_2SO_4 solution) and the inorganic intercalation compounds as both the cathode and anode. The use of aqueous electrolyte can not only fundamentally resolve the safety problem, but also endow the ARLB with many other advantages such as low cost, high power density, easy fabrication, and environmental friendliness. However, aqueous electrolyte imposes more requirements on the cathode and anode due to its narrow electrochemical window.

Till now, most pioneer work on ARLB used layered $LiCoO_2$ or spinel $LiMn_2O_4$ as the cathode for ARLB. The anode candidates were usually V or Ti based oxides and compounds, such as VO_2 [1], LiV_3O_8 [2–9], $Li_xV_2O_5$ [10], V_2O_5 [11], TiP_2O_7 [12] and $LiTi_2(PO_4)_3$ [12–14] mainly because of their redox potential being between 2 and 3 V vs Li^+/Li. Although much improvement in energy density has been achieved comparing with the first ARLB, unfortunately, these inorganic anode materials still show low specific capacity and

* Corresponding author. Tel.: +86 27 68756931; fax: +86 27 68754067.
E-mail address: zhanhui3620@126.com (H. Zhan).
[1] These authors contributed equally to this work.

0378-7753/$ – see front matter © 2013 Elsevier B.V. All rights reserved.
http://dx.doi.org/10.1016/j.jpowsour.2013.10.091

unsatisfactory working voltage in the aqueous electrolyte, resulting in low energy density of the ARLB. In addition, the cycling stability of ARLB is also very poor, due to the poor stability of anode in aqueous electrolyte. Many researches have proved that it is caused by the side reaction of anode with water and/or oxygen [14], the dissolution of active material in electrolyte [8], as well as the unfavorable structural change during the charge/discharge process. It is concluded that the development of ARLB is seriously restricted by the electrochemical performance of anode material.

To circumvent this problem, recently, researchers attempted to use active carbon [15] or polypyrrole (PPy) [16] instead of inorganic intercalation compounds as the anode for ARLB. For PPy, its redox process involves the doping/de-doping reaction of polymer. As its capacity is greatly limited by the doping degree, the practical capacity is usually no more than 80 mAh g^{-1}. In addition, its high redox potential, averagely −0.4 V vs SCE [16], further lower the energy density. For the active carbon, the capacitance property of carbon is utilized, so its cycle life is excellent, namely as long as more than 20,000 cycles [15]. Although using carbon anode substantially avoid the structural degradation and the side reaction with electrolyte during the charging/discharging, they also lead to much lower energy density because of the capacitance nature of carbon anode. Additionally, the capacitance behavior of carbon anode brings about a rather sloping charge/discharge profile of the carbon/$LiMn_2O_4$ full cell [15], which eventually harms the energy density property. How to obtain higher energy density and longer cycle life for ARLB simultaneously is a critical issue for the development of ARLB.

Here an alternative approach is proposed to use the electroactive organic material with conjugated carbonyl group as the anode for ARLB. Comparing with previously reported anode material for ARLB, Polyimide anode has a totally different redox mechanism (Fig. 1). Unlike the commonly known intercalation mechanism or doping/de-doping mechanism, it can undergo an enolization process when combining with cation with +1 charge

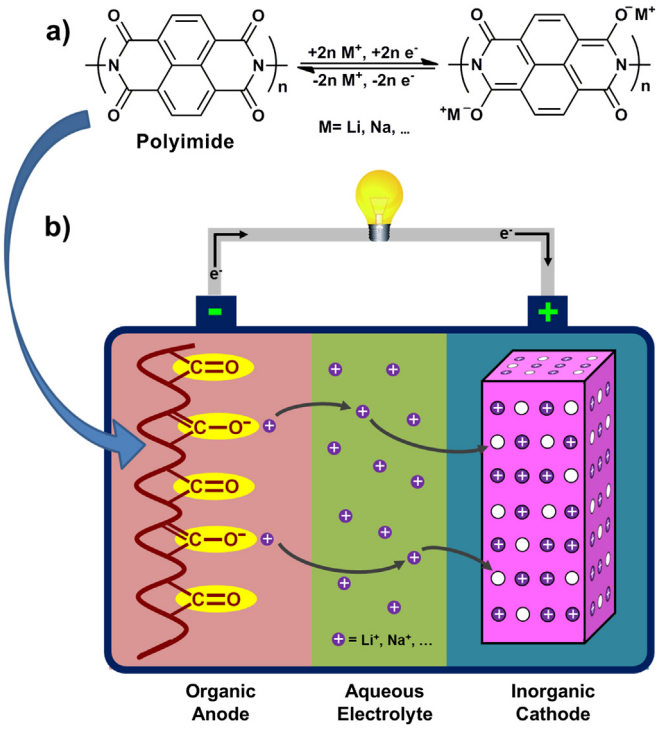

Fig. 1. a) The electrochemical redox mechanism of Polyimide; b) The cell configuration and operating principle of aqueous rechargeable alkali ion battery based on the organic anode with conjugated carbonyl group and the inorganic intercalation cathode.

state, accompany with the charge redistribution within the conjugated aromatic molecule. During the process, the polymer framework keeps intact. The different mechanism endows Polyimide with excellent structural stability and fast reaction kinetics. Since Li^+ is not indispensable for the electrochemical redox reaction of this organic anode (Fig. 1), its application can be extended to other battery systems, for example, aqueous rechargeable sodium-ion battery (ARSB). Therefore, in general, we call this novel battery system as "Aqueous Rechargeable Alkali-ion Battery".

In this paper, ARLB and ARSB are demonstrated by Polyimide/$LiCoO_2$ and Polyimide/$NaVPO_4F$ cell respectively. The Polyimide anode material has 1,4,5,8-naphthalenetetracarboxylic dianhydride (NTCDA) moiety. Their electrochemical property has been studied in terms of cyclic voltammetry and charging/discharging tests. The excellent electrochemical performance of Polyimide in both $LiNO_3$ and $NaNO_3$ solution, as well as the structural diversity of organic material, give an important insight in developing a new generation of aqueous rechargeable alkali-ion battery.

2. Experimental

2.1. Synthesis

For the synthesis of Polyimide, *N*, *N*′-diamino-1,4,5,8-naphthalenetetracarboxylic bisimide (DANTCBI) was prepared first as an intermediate [17,18]. 1,4,5,8-naphthalenetetracarboxylic bisimide (NTCDA) was dissolved in boiling ethanol, and a slightly excess amount of hydrazine hydrate was added. The hot mixture was filtrated and the solid product was vacuum dried at 80 °C. Thus obtained DANTCBI intermediate further reacted with NTCDA under reflux in *p*-chlorophenol solvent for 6 h. The product was filtrated, washed with ethanol for several times, dried at 120 °C in air for 12 h, and then heated at 350 °C for 8 h in N_2 flow to obtain the final product.

$LiCoO_2$ was prepared by a commonly used high-temperature calcination method [19]. The mixture of stoichiometric Li_2CO_3 and Co_3O_4 was heated at 850 °C for 5 h and then annealed at 920 °C for another 5 h.

$NaVPO_4F$ was prepared by a sol–gel method [20]. V_2O_5 and oxalic acid were dissolved in ethanol, and then stirred at 80 °C until the color of solution turned into green. Stoichiometric $NH_4H_2PO_4$ and NaF were added with continuous stirring. A green sol mixture was formed and then vacuum dried at 80 °C for 24 h. Finally, the gel precursor was grounded and heated in a tube furnace at 800 °C for 6 h under flowing N_2.

2.2. Electrode preparation and testing

The composition of electrode is as follows. For Polyimide electrode, it was composed of Polyimide, Printex XE2 carbon and PTFE binder with the mass ratio of 6: 3: 1; for $LiCoO_2$ electrode, it contained 80 wt% $LiCoO_2$, 10 wt% acetylene black (50% compressed, xinglongtai chemical Co., LTD., Tianjin, China) and 10 wt% PTFE; while for $NaVPO_4F$, it comprised 60 wt% $NaVPO_4F$, 30 wt% acetylene black and 10 wt% PTFE. Stainless steel mesh was used as the current collector. 5 M $LiNO_3$ solution and 5 M $NaNO_3$ solution were used as the electrolyte for ARLB and ARSB respectively.

For the three-electrode cell, a saturated calomel electrode (SCE, E = 0.2415 V vs SHE, or E = 3.29 V vs Li^+/Li) was used as the reference electrode, and excess $LiCoO_2$, $NaVPO_4$ or polyimide material was used as the counter electrode. For example, when the working electrode was $LiCoO_2$, the counter electrode was excess Polyimide, and vice versa. The three-electrode cell was used in CV test and the cycling test of Polyimide, $LiCoO_2$, $NaVPO_4F$ electrode. In the full cell evaluation, the anode and cathode was separated by a

glass fiber separator (whatman, GF/B) in CR2016 coin cell. Both the three-electrode cell and coin cell were assembled in open environment. LAND battery cycler (China) was used for the cycling test and the CV tests were conducted on AUTOLAB electrochemical workstation (Netherlands).

All electrochemical measurements were performed at ambient temperature.

3. Results and discussion

The pH value was chosen as 7 in our test, because previous study and our experiments showed that lower pH value would cause proton insertion into $LiCoO_2$ and thus-resulted property deterioration [21,22], while higher pH value leaded to more occurrence of the side reaction and thus low columbic efficiency.

Fig. 2a shows the cyclic voltammogram of $LiCoO_2$ and Polyimide electrode in 5 M $LiNO_3$ solution, and the H_2/O_2 evolution voltammetry is also presented as the background. It can be seen that the electrochemical stability window of 5 M $LiNO_3$ solution locates within −0.7–1.2 V vs SCE. The CV curve of $LiCoO_2$ in 5 M $LiNO_3$ electrolyte indicates that $LiCoO_2$ can be completely oxidized without significant O_2 evolution, corresponding well with previous observation on $LiCoO_2$ electrode in $LiNO_3$ solution [21,22]. The two pairs of redox peaks at 0.78/0.70 V and 0.89/0.88 V vs SCE indicates different phase transformation upon Li^+ insertion/de-insertion [15].

Polyimide can be completely reduced just before H_2 evolution as shown in Fig. 2a, with a pair of symmetric redox peaks at −0.34/-0.52 V vs SCE. The location of the redox peaks resembles well with 2.75/2.55 V vs Li^+/Li in nonaqueous electrolyte in our previous observation [31], indicating the formation of carbonyl di-anion (see Fig.1a). The result in Fig. 2a suggests that using Polyimide anode and $LiCoO_2$ cathode can effectively utilize the electrochemical window of $LiNO_3$ solution, and lead to high working voltage and thus high energy density.

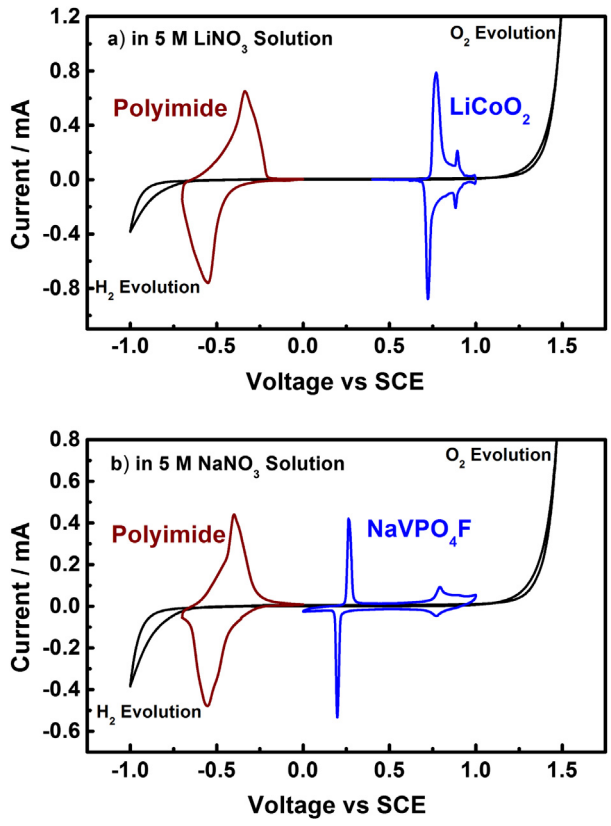

Fig. 2. CV curves of a) Polyimide and $LiCoO_2$ in 5 M $LiNO_3$ solution and b) Polyimide and $NaVPO_4F$ in 5 M $NaNO_3$ solution at a scan rate of 0.1 mV s^{-1}.

To further verify the viability of ARSB concept, the cyclic voltammogram of $NaVPO_4F$ and polyimide electrode in 5 M $NaNO_3$ was collected. As concerns the cathode, although many cathode materials for Na-ion batteries have been reported [23], including sodium transitional metal oxides (e.g., Na_xCoO_2 [24,25] and Na_xMnO_2 [26,27]), phosphates (e.g., $NaFePO_4$ and $Na_3V_2(PO_4)_3$) and fluorophosphates (e.g., $NaVPO_4F$ [20,28] and $Na_3V_2(PO_4)_2F_3$), their electrochemical performance is still not comparable to the cathode for Li-ion batteries. $NaVPO_4F$ is finally chosen in our study, because it has already shown a relatively flatter discharging plateau and a good cycling stability in nonaqueous electrolyte [23]. In 5 M $NaNO_3$ aqueous electrolyte, $NaVPO_4F$ showed two pairs of redox peaks at 0.26/0.20 V and 0.79/0.77 V vs SCE, locating at the left side of O_2 evolution (Fig. 2b), which corresponds to the two different insertion/de-insertion process of $NaVPO_4F$ [23].

In Fig. 2b, it is observed that the cyclic voltammogram of Polyimide electrode in 5 M $NaNO_3$ solution is quite similar to that in 5 M $LiNO_3$ solution. It showed a pair of symmetric redox peaks at −0.40/−0.55 V vs SCE, corresponding to 2.22/2.07 V and 2.47/2.27 V vs. Na^+/Na (not shown here), exactly above the H_2 evolution potential (−0.7 V vs SCE). The result is understandable if the redox reaction nature of Polyimide is considered. As being mentioned above, different from other inorganic intercalation electrode material with rigid crystal structure, whose electrochemical property especially the intercalation reaction kinetics is greatly related to the ionic radius of insertion ion and the interspace within crystallite, the very flexible polymer framework of Polyimide greatly facilitates the ion transport, thus the type of cation (Li^+ or Na^+) will not significantly impact the reaction kinetics. From the result in Fig. 2b, it can be concluded that both Polyimide anode and $NaVPO_4F$ cathode are compatible with $NaNO_3$ solution.

The capacity performance of $LiCoO_2$ cathode and Polyimide anode in 5 M $LiNO_3$ solution is tested using a three-electrode cell with SCE as the reference electrode. At the current density of 100 mA g^{-1}, $LiCoO_2$ can deliver a discharge capacity of 129 mAh g^{-1} between 0 and 1.0 V (Fig. 3a) with an average discharging voltage of 0.75 V vs. SCE. The coulomb efficiency in the first cycle is as high as 98.4% (Fig. 3a), which indicates very insignificant side reaction in the first cycle. The capacity performance is very close to previous report of $LiCoO_2$ in $LiNO_3$ solution [21,22].

From the 1st charge/discharge profile of Polyimide anode (Fig. 3b), its average discharging and charging voltage was −0.50 and −0.39 V vs SCE respectively, and it delivered a discharging capacity of 192 mAh g^{-1} and a charging capacity of 160 mAh g^{-1}. The capacity gap between the discharging and charging process should be ascribed to the irreversible reduction of residual O_2 on the anode in aqueous solution. In our test, an open three-electrode cell with large volume of aqueous solution was used and no further deaerating treatment was conducted prior to the test, so the impact of residue O_2 cannot be ignored. This phenomenon was also observed on many other inorganic anode materials for ARLB [2,10,12,14]. However, the adverse impact will be greatly reduced in our full cell because of the sealed cell configuration and the much smaller amount of aqueous electrolyte and residue O_2. Another point needs to be noted is that the charging/discharging plateau of Polyimide is very flat, corresponding well with the sharp redox peaks in Fig. 2a. It is very different from the observation on carbon anode, whose charging/discharging profile is very sloping due to the capacitance reaction nature [29,30]. According to the capacity of $LiCoO_2$ (129 mAh g^{-1}) and Polyimide (160 mAh g^{-1}), it can be predicted that the maximum specific capacity of Polyimide/$LiCoO_2$

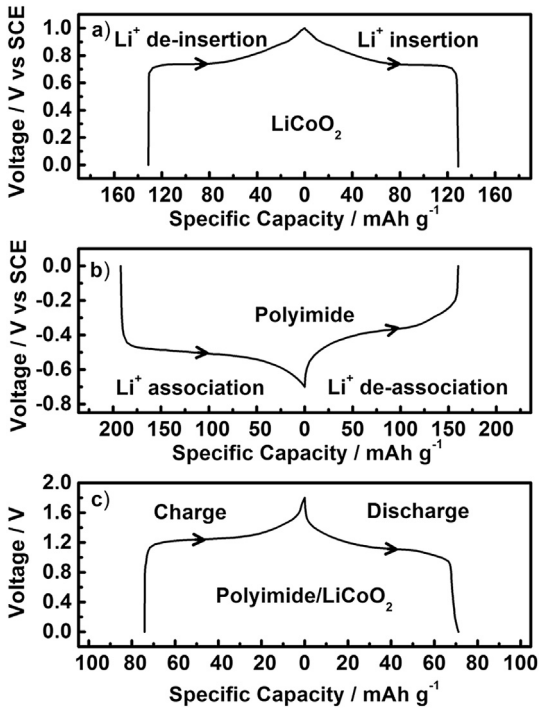

Fig. 3. Charge/discharge curves in the first cycle of a) $LiCoO_2$ electrode, b) Polyimide electrode and c) Polyimide/$LiCoO_2$ full-cell in 5 M $LiNO_3$ aqueous electrolyte at a current density of 100 mA g^{-1}. The cutoff voltage is 0–1.0 V vs SCE for a), 0 ~ −0.7 V vs SCE for b), and 0–1.8 V for c), respectively. The specific capacity of full-cell is calculated based on the weight of $LiCoO_2$ plus Polyimide.].

full cell is 71 mAh g^{-1} (based on the weight of $LiCoO_2$ plus Polyimide).

In order to evaluate the battery performance of Polyimide/$LiCoO_2$ full cell, CR2016 coin-cell was assembled. The mass ratio of $LiCoO_2$:Polyimide is set as 1.2 according to the 1st discharging capacity of $LiCoO_2$ and the 1st charging capacity of Polyimide (160:129 ≈ 1.2). In Fig. 3c, Polyimide/$LiCoO_2$ full cell shows an average discharging voltage of 1.12 V and a discharging capacity of 71 mAh g^{-1} in the first cycle, both of which are almost the same as being predicted above. The result indicates that the cathode as well as the anode active material is fully utilized in our Polyimide/$LiCoO_2$ full cell. Additionally, the rather flat charging/discharging plateau of the Polyimide/$LiCoO_2$ full cell is another advantage over many other ARLB systems.

Besides the energy density, we are also concerned with the cycling stability and rate capability of the Polyimide/$LiCoO_2$ cell. A step-wise cycling test was conducted and the result is shown in Fig. 4a. When the current density increased from 100 mA g^{-1} to 500 mA g^{-1}, the discharging capacity decreased from 71 mAh g^{-1} to 65 mAh g^{-1}, with an 8% capacity drop, indicating Polyimide/$LiCoO_2$ cell can well sustain high-rate charging/discharging. In Fig. 4b, we present the long-term cycling property of Polyimide/$LiCoO_2$ full-cell at a constant current density of 500 mA g^{-1}. The discharge capacity is 70 mAh g^{-1} in the first cycle and then slowly drops to 56 mAh g^{-1} at the 200th cycle, with the capacity retention of 80%. In addition, the coulomb efficiency is well maintained at above 99% after the initial several cycles.

In Fig. 5, the electrochemical performance of three typical ARLB systems is compared. They are composed of intercalation cathode and anode with different reaction mechanism. For example, $LiTi_2(PO_4)_3$/$LiMn_2O_4$ use intercalation compound of $LiTi_2(PO_4)_3$ as anode, C/$LiMn_2O_4$ use capacitance material of carbon as anode, while our Polyimide/$LiCoO_2$ use organic carbonyl material of polyimide as anode.

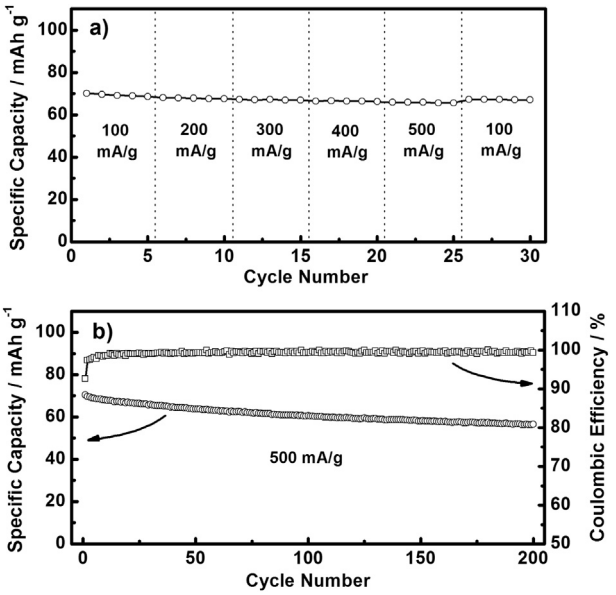

Fig. 4. Cycling profiles of Polyimide/$LiCoO_2$ full-cell a) at different current densities and b) at a constant current density of 500 mA g^{-1} (the capacity of full-cell is calculated based on the weight of $LiCoO_2$ plus Polyimide, the current density is determined by the mass of $LiCoO_2$). The cutoff voltage is 0–1.8 V.

Although the comparison is not very rigorous considering the slight inconsistency in cell fabrication and electrochemical test conditions, we can still conclude that our Polyimide/$LiCoO_2$ cell present the best comprehensive battery performance among all the ARLB systems. It has the highest specific capacity and specific energy density, as well as good cycling stability and rate capability. We should ascribe all these merits mainly to the organic anode material. First, Polyimide anode can deliver much higher charge capacity than carbon anode even other inorganic intercalation anode materials in aqueous electrolyte. For example, the practical capacity of 200 mAh g^{-1} in nonaqueous electrolyte [31] or the capacity of 160 mAh g^{-1} in aqueous $LiNO_3$ electrolyte (restricted by the electrochemical window of $LiNO_3$ solution) are both much higher than carbon anode and the inorganic intercalation anode materials (<100 mAh g^{-1}), such as LiV_3O_8 [2,10], TiP_2O_7 and $LiTi_2(PO_4)_3$ [12]. More importantly, Polyimide anode has a relatively lower average charge voltage as well as a rather flat discharge plateau especially comparing with the carbon anode, which enables the full utilization of $LiCoO_2$ cathode and eventually leads to a higher working voltage of the full cell. Second, Polyimide is intrinsically more stable than the intercalation inorganic compound with rigid crystal

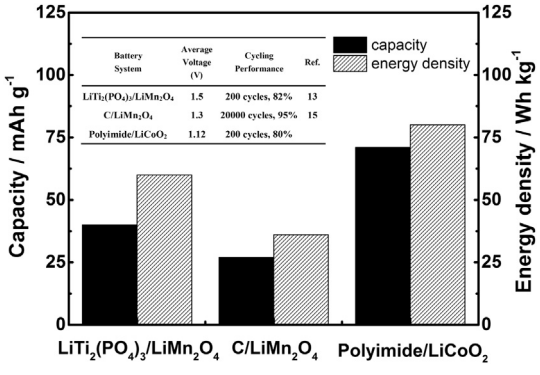

Fig. 5. Comparison of the battery performance of three typical ARLB systems.

lattice. Finally, the flexible polymer backbone and the fast redox kinetics of conjugated carbonyl group [32] endow Polyimide with excellent rate capability.

As being mentioned above, the electrochemical behavior of Polyimide anode is not affected by the type of cation (Li^+ or Na^+), and the feasibility of Polyimide/$NaVPO_4F$ ARSB system has already been verified by CV measurement. In Fig. 6, it shows the electrochemical performance of Polyimide anode, $NaVPO_4F$ cathode and Polyimide/$NaVPO_4F$ full cell in $NaNO_3$ solution. The test condition is as same as that for ARLB. As shown in Fig. 6a, $NaVPO_4F$ cathode can deliver an initial discharge capacity of 54 mAh g^{-1} in 5 M $NaNO_3$ solution, with two voltage plateaus at 0.8 V and 0.2 V vs SCE. The result is reasonable because although the theoretical capacity of $NaVPO_4F$ is as much as 143 mAh g^{-1}, its practical capacity in nonaqueous electrolyte is only about 80 mAh g^{-1} in previous report [28] because of the slow Na^+ intercalation chemistry. In our experiment, the capacity further decreases to 54 mAh g^{-1} because relatively higher current rate applied.

For Polyimide anode, the discharging and charging capacity in 5 M $NaNO_3$ solution is 184 and 165 mAh g^{-1} respectively, which is very close to that in $LiNO_3$ solution. The observation further indicates that the cation type will not impact the capacity performance of polyimide anode. Similar result has been gained on another organic analog, Zhao [33] and Park [34] both get ~250 mAh g^{-1} capacity on $Na_2C_8H_4O_4$ in nonaqueous Na^+ electrolyte, which was very close to $Li_2C_8H_4O_4$ in Li^+ electrolyte [35]. Based on the discharging capacity of $NaVPO_4F$ (54 mAh g^{-1}) and the charging capacity of Polyimide (165 mAh g^{-1}), the maximum capacity of polyimide/$NaVPO_4F$ cell should be 41 mAh g^{-1}. In Fig. 6c, our Polyimide/$NaVPO_4F$ full cell (mass ratio of Polyimide: $NaVPO_4F$ was 3.1) shows an initial capacity of 40 mAh g^{-1}. Obviously, the capacity performance of Polyimide/$NaVPO_4F$ full cell is not as good as Polyimide/$LiCoO_2$ cell. In Fig. 7, the cycling behavior of Polyimide/$NaVPO_4F$ full cell is presented, the capacity decreased from

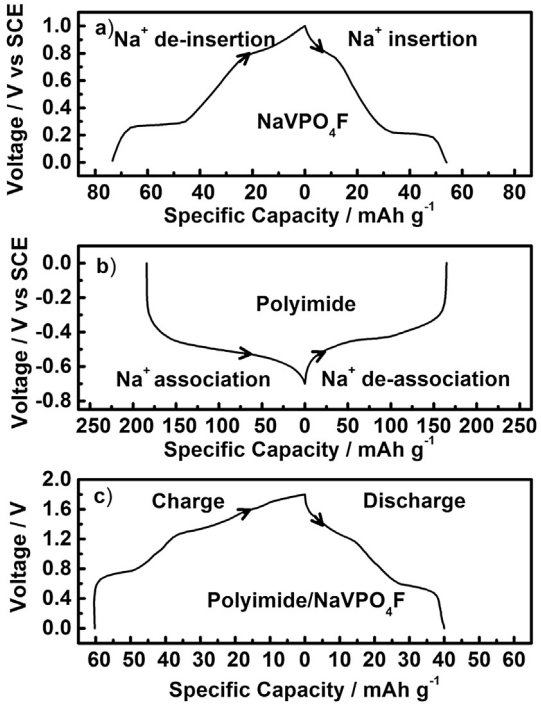

Fig. 6. Charge/discharge curves in the first cycle of a) $NaVPO_4F$ electrode, b) Polyimide electrode and c) Polyimide/$NaVPO_4F$ full-cell in 5 M $NaNO_3$ aqueous electrolyte at a current density of 50 mA g^{-1}.The cutoff voltage is 0–1.0 V vs SCE for a), 0 ~ −0.7 V vs SCE for b), and 0–1.8 V for c), respectively. The capacity of full-cell is calculated based on the weight of $NaVPO_4F$ plus Polyimide.

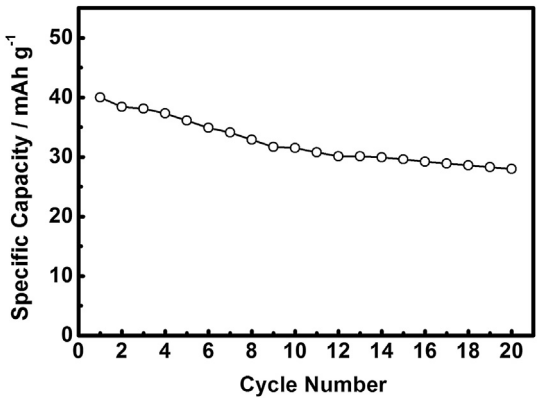

Fig. 7. Cycling profiles of Polyimide/$NaVPO_4F$ full-cell at a current density of 50 mA g^{-1} (the capacity of full cell is calculated based on the weight of $NaVPO_4F$ plus Polyimide, the current density is determined by the mass of $NaVPO_4F$). The cutoff voltage is 0–1.8 V.

40 mAh g^{-1} in the 1st cycle to about 30 mAh g^{-1} in the 20th cycle. From the results shown in Figs. 4 and 7, we can see the electrochemical performance of Polyimide/$NaVPO_4F$ cell is poorer than that of Polyimide/$LiCoO_2$ cell. However, we have to ascribe the inferior full-cell performance of ARSB mainly to the $NaVPO_4F$ cathode instead of the Polyimide anode. Fig. 8 gives the result of cycling test of $NaVPO_4F$ and Polyimide electrode in 5 M $NaNO_3$ solution. It can be seen that $NaVPO_4F$ electrode presents much worse capacity retention than Polyimide electrode. Within 20 cycles, about 30% capacity drop is observed on $NaVPO_4F$ electrode, while less than 17% capacity decay occurs on Polyimide electrode (it

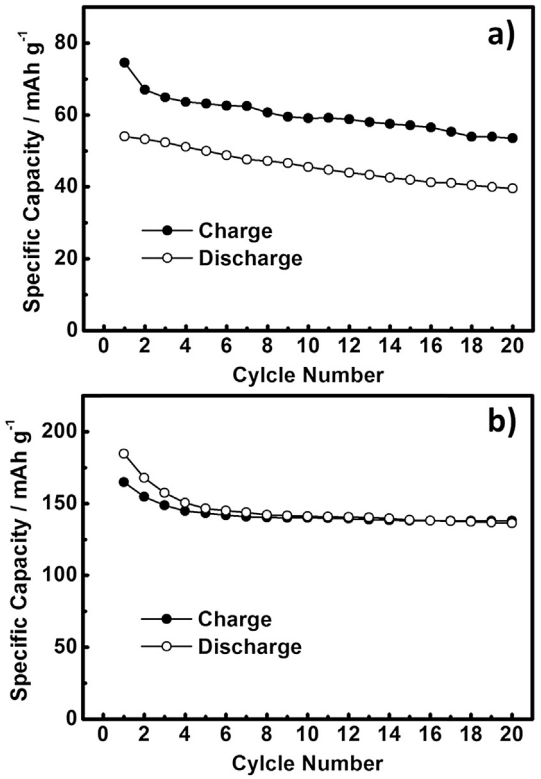

Fig. 8. The cycling profiles of $NaVPO_4F$ a) and Polyimide b) in 5 M $NaNO_3$ solution at a current density of 50 mA g^{-1}. The cutoff voltage is 0 ~ −0.7 V vs SCE for a) and 0–1.0 V vs SCE for b).

has to be pointed out that the capacity decay of polyimide electrode is attributed to the effect of residue O_2. In our study, no deaerating treatment was conducted prior to the test, and it definitely would lead to capacity degradation according to previous study [14]). As a demonstration of ARSB, although the capacity performance of Polyimide/$NaVPO_4F$ system is not very satisfactory, we still certainly believe that Polyimide is a good anode material for not only ARLB, but also ARSB. A more successful ARSB system can be expected, depending on the development of cathode materials for Na-ion batteries, such as recently reported $Na_3V_2(PO_4)_3$ [36].

4. Conclusion

Electrochemical experiments prove the good cycling stability and compatibility of Polyimide in both $LiNO_3$ and $NaNO_3$ solution. Therefore, Polyimide anode is demonstrated as a high performance anode material for both ARLB and ARSB. Due to a more appropriate redox potential, higher specific capacity, different redox mechanism and very stable structure, the Polyimide/$LiCoO_2$ system achieved the highest capacity and energy density among all the ARLB systems, namely a specific capacity of 71 mAh g^{-1} and a specific energy density of 80 Wh kg^{-1}. In addition, it showed high coulomb efficiency, excellent cycling stability and rate capability. The electrochemical performance of Polyimide/$NaVPO_4F$ battery was not as good as Polyimide/$LiCoO_2$ cell, because the poor capacity and poor cycling stability of $NaVPO_4F$ cathode deteriorate the full cell property. Encouraged by the excellent electrochemical performance of Polyimide anode in both $LiNO_3$ and $NaNO_3$ solution and the fact that organic material has very diversified structure, we believe that more aqueous rechargeable alkali-ion battery can be developed by exploring other organic materials.

Acknowledgments

Authors would express their sincere thanks to the Nature Science Foundation of China (No. 21073138, 21273168, 21233004) for the financial support.

References

[1] W. Li, J.R. Dahn, D.S. Wainwright, Science 264 (1994) 1115–1117.
[2] J. Kohler, H. Makihara, H. Uegaito, H. Inoue, M. Toki, Electrochim. Acta 46 (2000) 59–65.
[3] G.J. Wang, L.J. Fu, N.H. Zhao, L.C. Yang, Y.P. Wu, H.Q. Wu, Angew. Chem. Int. Ed. 46 (2007) 295–297.
[4] G.J. Wang, N.H. Zhao, L.C. Yang, Y.P. Wu, H.Q. Wu, R. Holze, Electrochim. Acta 52 (2007) 4911–4915.
[5] G.J. Wang, H.P. Zhang, L.J. Fu, B. Wang, Y.P. Wu, Electrochim. Commun. 9 (2007) 1873–1876.
[6] G.J. Wang, L.J. Fu, B. Wang, N.H. Zhao, Y.P. Wu, R. Holze, J. Appl. Electrochem. 38 (2008) 579–581.
[7] G.J. Wang, Q.T. Qu, B. Wang, Y. Shi, S. Tian, Y.P. Wu, R. Holze, J. Power Sources 189 (2009) 503–506.
[8] A. Caballero, J. Morales, O.A. Vargas, J. Power Sources 195 (2010) 4318–4321.
[9] M.S. Zhao, Q.Y. Zheng, F. Wang, W.M. Dai, X.P. Song, Electrochim. Acta 56 (2011) 3781–3784.
[10] H.B. Wang, Y.Q. Zeng, K.L. Huang, S.Q. Liu, L.Q. Chen, Electrochim. Acta 52 (2007) 5102–5107.
[11] I. Stojkovic, N. Cvjeticanin, I. Pašti, M. Mitric, S. Mentus, Electrochem. Commun. 11 (2009) 1512–1514.
[12] H.B. Wang, K.L. Huang, Y.Q. Zeng, S. Yang, L.Q. Chen, Electrochim. Acta 52 (2007) 3280–3285.
[13] J.Y. Luo, Y.Y. Xia, Adv. Funct. Mater. 17 (2007) 3877–3884.
[14] J.Y. Luo, W.J. Cui, P. He, Y.Y. Xia, Nat. Chem. 2 (2010) 760–765.
[15] Y.G. Wang, Y.Y. Xia, J. Electrochem. Soc. 153 (2006) A450–A454.
[16] G.J. Wang, L.C. Yang, Q.T. Qu, B. Wang, Y.P. Wu, R. Holze, J. Solid State Electrochem. 14 (2010) 865–869.
[17] R.A. Dine-Hart, J. Polym. Sci. 6 (1968) 2755–2764.
[18] H. Ghassemi, A.S. Hay, Macromolecules 27 (1994) 3116–3118.
[19] J.P. Yu, X.H. Hu, H. Zhan, Y.H. Zhou, J. Power Sources 189 (2009) 697–701.
[20] J.Q. Zhao, J.P. He, X.C. Ding, J.H. Zhou, Y.O. Ma, S.C. Wu, R.M. Huang, J. Power Sources 195 (2010) 6854–6859.
[21] R. Ruffo, C. Wessells, R.A. Huggins, Y. Cui, Electrochem. Commun. 11 (2009) 247–249.
[22] R. Ruffo, F.L. Mantia, C. Wessells, R.A. Huggins, Y. Cui, Solid State Ionics 192 (2011) 289–292.
[23] V. Palomares, P. Serras, I. Villaluenga, K.B. Hueso, J. Carretero-Gonzalez, T. Rojo, Energy Environ. Sci. 5 (2012) 5884–5901.
[24] Y.P. Ma, M.M. Doeff, S.J. Visco, L.C.D. Jonghe, J. Electrochem. Soc. 140 (1993) 2726–2733.
[25] R. Berthelot, D. Carlier, C. Delmac, Nat. Mater. 10 (2011) 74–80.
[26] A. Caballero, L. Hernan, J. Morales, L. Sanchez, J.S. Pena, M.A.G. Aranda, J. Mater. Chem. 12 (2002) 1142–1147.
[27] Y.L. Cao, L.F. Xiao, W. Wang, D. Choi, Z. Nie, J. Yu, L.V. Saraf, Z. Yang, J. Liu, Adv. Mater. 23 (2011) 3155–3160.
[28] J. Barker, M.Y. Saidi, J.L. Swoyer, Electrochem. Solid-State Lett. 6 (2003) A1–A4.
[29] J.W. Long, D. Belanger, T. Brousse, W. Sugimoto, M.B. Sassin, O. Crosnier, MRS Bull. 36 (2011) 513–522.
[30] Q.T. Qu, Y. Shi, S. Tian, Y.H. Chen, Y.P. Wu, R. Holze, J. Power Sources 194 (2009) 1222–1225.
[31] Z.P. Song, H. Zhan, Y.H. Zhou, Angew. Chem. Int. Ed. 49 (2010) 8444–8448.
[32] Z.P. Song, T. Xu, M.L. Gordin, Y.-B. Jiang, I.-T. Bae, Q.F. Xiao, H. Zhan, J. Liu, D.H. Wang, Nano Lett. 12 (2012) 2205–2211.
[33] L. Zhao, J. Zhao, Y.-S. Hu, H. Li, Z.B. Zhou, M. Armand, L.Q. Chen, Adv. Energy Mater. 2 (2012) 962–965.
[34] Y. Park, D.-S. Shin, S.H. Woo, N.S. Choi, K.H. Shin, S.M. Oh, K.T. Lee, S.Y. Hong, Adv. Mater. 24 (2012) 3562–3567.
[35] M. Armand, S. Grugeon, H. Vezin, S. Laruelle, P. Ribière, P. Poizot, J.-M. Tarascon, Nat. Mater. 8 (2009) 120–125.
[36] Z.L. Jian, L. Zhao, H. Pan, Y.-S. Hu, H. Li, W. Chen, L.Q. Chen, Electrochem. Commun. 14 (2012) 86–89.